HHS Public Access

Author manuscript

Parasite Immunol. Author manuscript; available in PMC 2018 August 01.

Published in final edited form as:

Parasite Immunol. 2017 August ; 39(8): . doi:10.1111/pim.12441.

Antecedent *Nippostrongylus* infection alters the lung immune response to *Plasmodium berghei*

JM Craig[1] and **AL Scott**[1]

[1]W. Harry Feinstone Department of Molecular Microbiology and Immunology, Johns Hopkins Bloomberg School of Public Health, Baltimore, MD

Abstract

In endemic regions, it is not uncommon for patients to be co-infected with soil-transmitted helminthes and malaria. Although both malaria and many helminth species use the lungs as a site of development, little attention has been paid to the impact that pulmonary immunity induced by one parasite has on the lung response to the other. To model the consequences of a prior hookworm exposure on the development of immunity to malaria in the lungs, mice were infected with *Nippostrongylus brasiliensis* and two weeks later challenged with *Plasmodium berghei*. We found that a preexisting hookworm-induced Type 2 immune environment had a measurable but modest impact on the nature of the malaria-driven Type 1 cytokine response in the lungs that was associated with a transient effect on parasite development and no significant changes in morbidity and mortality after malaria infection. However, prior hookworm infection did have a lasting effect on lung macrophages, where the malaria-induced M1-like response was blunted by previous M2 polarization. These results demonstrate that, although helminth parasites confer robust changes to the immunological status of the pulmonary microenvironment, lung immunity is plastic and capable of rapidly adapting to consecutive heterologous infections.

Keywords

hookworm; malaria; lung; alveolar macrophage; M1; M2; emphysema

Introduction

The soil-transmitted nematodes *Ascaris lumbricoides*, *Trichuris trichiura*, *Necator americanus*, and *Ancylostoma duodenale* are among the most prevalent infections on earth, affecting ~2 billion of the poorest and most resource-deprived communities of sub-Saharan Africa, the Americas, and East Asia (1–3). A substantial proportion of helminth-infected individuals reside in areas that are also endemic for malaria, thus helminth-malaria co-infection is common (1, 4).

Correspondence: Alan L. Scott, PhD, W. Harry Feinstone Department of Molecular Microbiology and Immunology, Johns Hopkins Bloomberg School of Public Health, 615 N. Wolfe St., Room E5152, Baltimore, MD 21205, Tel.: 410-955-3430, ascott5@jhu.edu.

Disclosures: None. The authors have no conflicts of interest including financial interests in any company or institution.

Although the adult forms of the major helminthes are found in the intestine, the life cycles of these nematode species includes an obligate lung-stage of larval development marked by a programmed migration through the pulmonary vasculature and respiratory epithelium (5). The blood-borne larvae penetrate from the endothelium through the interstitium and into the alveolar space, causing tissue damage and initiating an inflammatory response. In areas of high transmission, patients experience extensive pulmonary damage that can result in respiratory distress (6). The immune response induced by parasitic helminths is characterized by a systemic and mucosal Th2 polarization typified by increases in IL-4, IL-13, IgE, eosinophilia, alternatively-activated (M2) macrophages, and Type 2 innate lymphoid cells (ILC2s) (7, 8). In addition, worm infections induce regulatory responses that control the level of parasite-induced pathology (9–12) that are sufficiently potent to have significant bystander effects on immunization, autoimmunity, and responses to other pathogen challenges (10, 11, 13, 14). *Nippostrongylus brasiliensis* has been used extensively as a model for human hookworm infection to study the immunology of the lung stage of infection. Despite establishing only a transient residence in the lungs (12–48 hours), *N. brasiliensis* larvae induce long-lived Th2/M2 skewing and structural changes to the lung environment (15–17) that can impact downstream immune responses to diverse challenges including infection and allergen exposure (13, 17–19). The M2-polarized resident macrophage population, in addition to its role in wound repair, has been shown to be important in protection against secondary challenge (15).

Malaria also establishes an important association with the lung environment. During the development of the asexual stage, infected erythrocytes adhere to the pulmonary microvasculature in large numbers (20–22). This transient sequestration in the lung prevents *Plasmodium*-infected cells from being cleared by immune mechanisms in the spleen and has the added benefit of promoting parasite growth (23, 24). This pulmonary sequestration has been implicated in the pathogenesis of malaria-associated acute lung injury (ALI) and acute respiratory distress syndrome (ARDS) in humans and mouse models (22, 25–27). In contrast to the strong Th2 immunity associated with nematode infections, malaria is characterized by elevated IL-12 and IFNγ and the expansion of $CD4^+$ Th1 cells, cytotoxic NK and $CD8^+$ T lymphocytes, and classically activated (M1) macrophages (28, 29). Monocytes and macrophages have also been shown to be important in clearing infected erythrocytes from the lung and controlling the level of malaria-induced inflammation(22).

Given the widespread occurrence of helminth-malaria polyparasitism and the highly divergent and counter-regulatory nature of the immune responses induced by these pathogens (30), it is of considerable interest to understand how preexisting infection with one influences the parasitemia and pathogenesis or the other. While a number of epidemiological and animal model studies have investigated helminth-malaria co-infections in terms of the impact on malaria systemic immunity, morbidity, and mortality (reviewed in (12, 31–33)), none have focused on the impact that a pre-existing nematode-induced Th2 polarization has on the parasitological and immunological dynamics of malaria infection in the lungs.

To address this issue, we infected BALB/cJ mice with *N. brasiliensis* to establish Th2/M2 polarization in the lungs prior to challenge with *Plasmodium berghei* ANKA. We found that

the robust Th2 cellular and cytokine environment established by hookworm infection is rapidly altered under the influence of the Th1-polarizing malaria infection. Despite this malaria-induced dampening of the pre-established pulmonary Th2 response, hookworm infection did have an impact on the activation phenotype of lung macrophages and on gross pathology. However, helminth-induced changes to the immunological status and the architecture of the lungs did not significantly influence the dynamics of malaria cytoadherence to lung vascular endothelial cells, morbidity, or mortality following *P. berghei* infection.

Materials and Methods

Animals

All experiments were performed using 8–10 week-old, male, wild-type BALB/cJ mice (Jackson Laboratories) under the approval of the Johns Hopkins University Animal Care and Use Committee. Mice were housed in a specific pathogen-free facility, continually provided filtered air and water, maintained on a 12-hour light/dark cycle, and fed autoclaved food *ad libitum*. All mice were anesthetized with a 450 mg/kg dose of avertin (*2,2,2*-tribromoethanol in *tert*-amyl alcohol, Sigma-Aldrich) diluted in phosphate-buffered saline (PBS) and administered via a 700 μL intraperitoneal injection prior to lung harvesting procedures.

Parasites and Infections

Infective-stage filariform (L3) *Nippostrongylus brasiliensis* larvae were isolated from rat fecal-charcoal-sphagnum moss cultures suspended over warm PBS in a modified Baermann apparatus as previously described (34). Larvae were washed three times in PBS and enumerated in an egg slide chamber (McMaster). Mice were infected subcutaneously in the scruff of the neck with 500 L3 larvae suspended in 200 μL PBS. All of the *N. brasiliensis*-infected animals, which expelled their adult parasites from the intestine at day 9–10 (data not shown), were subsequently infected with *P. berghei* ANKA on day 13.

The *Plasmodium berghei* ANKA strain MR4-671 was obtained from The Malaria Research and Reference Reagent Resource Center (MR4). Passaging and experimental infections of mice were established by a single 200 μL intraperitoneal injection containing 1×10^6 infected red blood cells diluted in PBS. Frozen MR4-617 stocks (20% v/v glycerol) were maintained at −80°C. To standardize experimental infections, parasites were flash-thawed in a 37°C water bath and serially passaged through at least two, but no more than eight, donor mice prior to experimental use. Blood from the donors was counted on a hemacytometer (Cambridge Instruments) to determine red blood cell density. Thin blood smears, fixed with 100% methanol and stained with 5% modified Giemsa (Sigma-Aldrich), were used to determine the percent parasitemia. After infection, parasitemia, core body temperature, and body weight were monitored daily using thin blood smears, a rectal thermometer probe (Physitemp), and a digital scale (Ohaus), respectively. Lungs were obtained on days 0, 3, 5, and 8 following malaria infection for cellular and molecular analyses.

Bronchoalveolar Lavage (BAL)

The trachea of anesthetized mice was cannulated and flushed three separate times with 1.0 mL of PBS. The recovered BAL fluids from each lavage were pooled and centrifuged to pellet the cells. After the supernatant was removed, the cells were suspended in 1.0 mL of PBS, counted on a hemacytometer (Cambridge Instruments), and adhered to a glass slide with the aid of cytology funnels (Fisher Scientific) and a CytoSpin centrifuge (Shandon). Cells were fixed and stained utilizing a DiffQuik™ kit (Andwin Scientific) for differential cell identification. Images of BAL cells were captured on a Nikon E800 microscope using the Spot Advanced camera and software (Diagnostic Instruments).

Lung Histology

Mice were anesthetized prior to tracheostomy and lungs were inflated at a constant pressure of 30 cmH_2O for 5 minutes with zinc-buffered formalin (Z-Fix, Anatech). The trachea was tied and the intact lungs were excised from the chest cavity and submerged in formalin for at least 48-hours. After fixation, lungs were randomly cut into 2–3 mm thick blocks, which were then embedded in paraffin. Five-micron sections were cut and stained with hematoxylin and eosin (H&E) and imaged on a Nikon E800 upright microscope using the Spot Advanced camera and software (Diagnostic Instruments).

Isolation of RNA and DNA from Whole Lung Homogenates

Mice were anesthetized prior to severing the abdominal aorta and perfusion of the lungs with 10 mL of PBS injected into the right ventricle of the heart. Lung tissues were homogenized in Trizol (Invitrogen), RNA was extracted with chloroform and purified with the PureLink™ RNA Mini Kit (Ambion), and DNA was precipitated from the remaining interphase/organic phase with 100% ethanol. The resulting DNA pellets were washed three times with 0.1 M sodium citrate in 10% ethanol, once with 75% ethanol, air-dried, and reconstituted in 8 mM NaOH adjusted to pH 8.4 with 1 M HEPES (Invitrogen).

Isolation of RNA and DNA from $CD11c^+$ Cells

Perfused lungs were removed, minced into fine pieces, and digested for 30 minutes in a 5 mL solution containing 1 mg/mL collagenase Type II (Invitrogen), 30 μg/mL DNase I (Roche Applied Science), and RPMI 1640 medium (Invitrogen). Tissues were ground through a 100 μm cell strainer (BD Biosciences) to form a single-cell suspension, washed, and suspended in ACK buffer (Invitrogen) to lyse red blood cells. The remaining leukocytes were passed through a 70 μm cell strainer (BD Biosciences), washed, and suspended in PBS containing 2% fetal calf serum (HyClone) and Fc Block™ (BD Biosciences) prior to surface staining with a CD11c-APC antibody (Miltenyi Biotec). Stained cells were washed and suspended in 50 μL of anti-APC-conjugated magnetic particles (IMag, BD Biosciences) for 30 minutes. After the addition of 1.0 mL of 0.5% bovine serum albumin (Sigma-Aldrich) and 2 mM EDTA (Invitrogen) in PBS, CD11c-APC^+ cells were purified by a cell separation magnet (BD Biosciences) following manufacturer's protocols. RNA was purified from isolated $CD11c^+$ cells with the use of a RiboPure Blood Kit (Ambion) and DNA was isolated utilizing the FlexiGene DNA kit (Qiagen) following manufacturer's instructions.

Real-Time PCR

Purified RNA and DNA concentrations were measured on a NanoDrop 1000 (Thermo Scientific). Either 500 ng of total RNA from $CD11c^+$ cells or 1.0 μg of total RNA from whole lung homogenates was reverse-transcribed with SuperScript II (Invitrogen) using Oligo-DT primer (Invitrogen) following manufacturer's protocols. The resulting cDNA was RNase H-treated (Invitrogen) prior to amplification following manufacturer's recommendations (Applied Biosystems). The following Assays-On-Demand primer-probe sets (Applied Biosystems) were used in this study: ADD PP SETSReactions were performed with the following thermal profile: 50°C for 2 minutes, 95°C for 10 minutes, and then 40 cycles of 95° C for 15 seconds followed by 60°C for 1 minute. Standard curves for each gene were constructed from the relative expression levels in 2-fold serial dilutions of pooled cDNAs from known positive samples. All samples were normalized to the housekeeping gene GAPDH. A similar protocol was followed for quantification of parasite DNA isolated from whole lungs or $CD11c^+$ cells using primers and probes specific to the *Plasmodium* 18s rRNA gene as previously described (35).

Statistical Analyses

The real-time RT-PCR results of changes to the expression levels of selected cytokine genes in the whole lungs were plotted as fold change over the average relative values obtained for naïve Day 0 animals after GAPDH normalization. Changes to the expression levels of selected cytokine genes determined by real-time RT-PCR analysis of $CD11c^+$ lung cells were plotted as relative values obtained from comparison to a standard curve for each gene after GAPDH normalization for all experimental days. The amount of *Plasmodium berghei* DNA detected in both whole lungs and $CD11c^+$ cells by real-time PCR was converted to number of parasites by assuming 0.02 pg is equivalent to a single parasite genome (36). All of the above data were converted to mean values ± standard error measurement (SEM) and analyzed in Prism (GraphPad) by two-way ANOVA with Bonferroni post-tests to compare all groups at each sample time. Comparisons of Kaplan-Meier survival curves between groups were analyzed by log-rank test using Prism software.

Results

Prior *N. brasiliensis* Infection has Only a Modest Impact on the Parasitemia, Morbidity and Mortality of Malaria Infection

It is well established that *N. brasiliensis* infection induces Th2 polarization of the lung characterized by a sustained increase in macrophages, a majority of which are M2 activated (17, 37). To test the hypothesis that this strong pre-existing Th2 environment alters the general course of a subsequent malaria infection, we compared the parasitological and physiological responses of age-matched BALB/cJ mice challenged with *P. berghei* alone (Pb) or with *P. berghei* 13 days following infection with *N. brasiliensis* (Nb/Pb). Although the rates of increase in parasitemia were comparable overall for the Pb and Nb/Pb groups, the Pb group had a somewhat higher percentage of infected erythrocytes at days 5 and 6 (Fig. 1A). While the Pb and Nb/Pb groups had a similar course of weight loss (Fig. 1B), the drop in body temperature of the Nb/Pb mice was more pronounced at days 7 and 8 (Fig. 1D) and this drop was associated with a trend toward an accelerated mortality (Fig. 1D). As

demonstrated previously (22), despite the continued rise in parasitemia, the burden of *P. berghei* in perfused lungs as measured by 18S rRNA, which was first detectable at day 3, peaked at day 5 of infection (Fig. 1E).

Histologically, as noted previously (22, 38), lungs from the Pb group showed modest pulmonary inflammation at day 5 characterized by an increase in cellular infiltration, focal edema and a marked alveolar septal thickening (Fig. 1F). This histological profile was maintained through day 8 (data not shown). The Nb/Pb group displayed the focal cellular infiltrates, emphysema-like loss of alveolar structure, and bronchiolar epithelial hyperplasia that is characteristic of the lungs during the post-expulsion phase of an Nb infection (16, 39, 40). While the Nb-associated histopathological changes were comparable in extent and intensity to that observed in the lungs from *N. brasiliensis*-only controls (Nb; Fig. 1F), the Nb/Pb lungs also had focal edema and thickened alveolar septa similar to the lungs from the Pb animals. Since the nature and extent of the histological changes in the Nb/Pb lungs appeared to simply reflect the additive contribution from the two parasites, we conclude that, over this narrow time window, sequential challenge with Nb and Pb does not result in a demonstrable change or acceleration in the overall nature or course of lung injury.

Nb-Induced Th2 Immunity Influences the Course of the Th1 Response to a Subsequent Malaria Infection

In addition to the strong systemic Th1 immune responses induced by Pb (41), Pb also induces a robust Th1-biased response in the lungs (42). To determine the impact that the Nb-induced Th2 skewing has on the lung-associated immune response to Pb, we monitored changes in the expression of genes involved in the induction and maintenance of Type 1 immune responses. Of the Th1-associated immune genes measured, only *il6* was modestly differentially expressed at day 0 of Pb infection (Fig. 2). While we found no significant differences in the expression dynamics of *il18, il12p35, and il12p40*, a prior Nb infection resulted in significantly lower *ifng* and reduced *il1b* expression on days 5 and 8 after Pb infection, respectively (Fig. 2). Although not statistically significant, we observed a similar trend for reduced expression of *tnf* and *nos2*. These data indicate that while the elements of the strong systemic Th1 response established by malaria (43) are detected in the Nb/Pb group, the magnitude of the Th1 response is somewhat blunted in the lung when it is Th2-skewed prior to malaria infection.

We also assessed the impact that malaria infection had on the established Nb-induced Th2 response in the lungs. Mice receiving Pb alone showed little change in the expression of *il33*, *il4*, and *il13*, as well as the markers for alternatively-activated (M2) macrophages *arg1* (Arginase 1), *chil3* (Chitinase 3-Like 3, YM1), and *retnla* (Resistin-Like Molecule Alpha, Relm-α, Fizz1) (Fig. 3). Of note is a transient increase in *il4* and *il13* expression in the Pb group at day 5 of infection. The lungs of mice that received Nb 13 days prior showed evidence of strong Th2 polarization with significantly elevated levels of all the Th2-associated genes (Fig. 3). As demonstrated previously (40, 44), the intensity of the expression of Th2-associated genes wanes as the cellular response to the acute lung damage caused by the Nb larvae resolves (Fig. 3). With initiation of malaria infection, the Nb/Pb

group also rapidly reduced the expression Th2-associated genes in the lungs with a kinetics that mirrored the Nb-only group (Fig. 3).

Tregs that produce IL-10 are crucial for establishing immune tolerance during a variety of challenges including helminth and malaria infections (45–47). In addition, IL-27, in concert with IL-21, has been shown to be required for regulating Th1-mediated inflammation through processes that involve both FoxP3$^+$ Treg and FoxP3$^-$ Tr1 cells in other organs (48). The differences in the levels of inflammatory markers between the Pb and Nb/Pb groups suggested that immunoregulatory cytokines might be differentially expressed. We found that both the Pb and Nb/Pb groups had comparable changes in the expression levels of *tgfb*, *il10*, *il27*, *il21* and *foxp3* (Fig. 4). Our data indicate that while these mechanisms are likely involved in the regulation of inflammatory responses to malaria in the lungs, they are not significantly altered by a prior hookworm infection.

Hookworm Infection Alters the Number, Gross Phenotype, and Activation Status of Lung Macrophages During A Subsequent Malaria Infection

Resident lung macrophages and recruited monocytes play key roles in controlling parasite numbers and homeostatic repair in both malaria and *N. brasiliensis* infections (15, 22, 37, 44). Therefore, we focused on identifying changes to the number and activation state of lung macrophage populations over the course of infection in the Pb, Nb and Nb/Pb lungs. As a consequence of Nb infection, the numbers of macrophages that were significantly elevated in the BALF from the Nb/Pb and Nb groups at day 0/13 dropped over the ensuing three days as the Nb-induced inflammation resolved (Fig. 5A). In contrast to the BALF-derived macrophages isolated at day 5 from the Pb group that had a morphological appearance similar to the cell lavaged from naïve animals (Fig. 5D), BAL-derived macrophages isolated from Nb/Pb animals appeared to be activated with a number of the cells containing dense granules similar to cells isolated from post-Nb lungs at a comparable time point (Fig. 5D).

Further, we characterized the dynamics and activation of the CD11c$^+$ alveolar and interstitial macrophage populations from the whole lung. Similar to dynamics in the BALF (Fig. 5A), the number of CD11$^+$ cells was significantly elevated on Day 0 in the lung from the Nb/Pb group and declined following Pb infection (Fig. 5B). Interestingly, in the Nb/Pb group, and to an even greater extent in the Pb alone group, the number of CD11c$^+$ cells increased substantially between Days 5 and 8 following malaria infection. The mean number of CD11c$^+$ macrophages at day 21 from the lungs of Nb group animals was 6.4×10^6 (data not shown). Utilizing a real-time PCR-based assay for detection of the *P. berghei* 18s rRNA gene, macrophages isolated from Nb/Pb lungs contained more than twice as many *P. berghei* genome equivalents on Day 5 compared to cells derived from the Pb lungs (Fig. 5C). This difference was no longer present on Day 8, when macrophages from the Pb lungs showed a substantial increase in phagocytic activity (Fig. 5C). We conclude that a previous hookworm infection primes lung-associated macrophages to affect a more rapid clearance of malaria-infected erythrocytes from the lungs compared to the cells from a malaria-only infection, but later in malaria infection this difference in phagocytic capacity is no longer evident.

To determine if this difference in the dynamics of parasite uptake was reflected in the activation status of the cells, bead-purified CD11c+ cells from Pb or Nb/Pb lungs were

analyzed for the expression of genes associated with classically-activated (M1), alternatively-activated (M2), and regulatory macrophages. It is important to note that whereas CD11c is a reliable surface marker for lung-resident macrophages, especially alveolar macrophages, other immune cells also express CD11c. The bead-based isolation protocol used in naïve animals resulted in cell preparations that were consistently ~95% lung-resident macrophages (data not shown). Previous and ongoing inflammation resulted in $CD11c^+$ cell preparations that, while still overwhelming dominated by resident and monocyte-derived macrophages, contained an increased and variable (from 8% to 17%) presence of recruited $CD11c^+$ DCs, NK cells, T cells, and B cells (data not shown).

On day 3 in the Pb group, $CD11c^+$ cells first increased expression of *il18*, a marker of inflammasome activation that has been shown to result from the uptake of *Plasmodium*-derived hemozoin, and *tgfb*, a regulatory cytokine important for controlling pulmonary inflammation (Fig. 6) (49, 50). Expression of these cytokine genes was then accompanied by increases in the levels of *tnf*, *il1b*, *il6*, *Iil27*, *nos2*, and *il10* on days 5 and 8 post-malaria infection. In contrast, despite carrying a heavier burden of Pb antigen on a per cell basis (Fig. 5C), phagocytic cells isolated from Nb/Pb lungs at day 5 of malaria infection had a significantly attenuated malaria-typic inflammatory signature and a marked increase in expression of the canonical M2-associated genes *arg1*, *chil3*, and *retnla* more consistent with that of an Nb-only infection (Fig. 6). Although 3 days later the malaria-typic response remained attenuated, the expression of M2 marker genes was significantly reduced. These data reveal that, in contrast to dominant Th1/M1 expression signature exhibited by the $CD11c^+$ cells isolated from the lungs of animals exposed to only Pb, cells isolated from lungs that had experienced a prior Nb infection maintain their M2 activation phenotype and dampen the malaria-induced Th1/M1 expression profile.

Discussion

The lungs are repetitively exposed to a diverse and complex amalgam of antigens and microbes inhaled from the environment as well as from the microbiome. This constant exposure necessitates a finely tuned immune response capable of identifying danger and balancing the intensity and duration of inflammation required to respond to a challenge with the appropriate levels of immune regulation, repair and remodeling to recover and maintain respiratory function. Infection history has an underappreciated impact on this complex process. Epidemiological and experimental evidence indicates that the innate and adaptive response to prior or concurrent pulmonary pathogens influences the immunological outcome to a subsequent challenge through alterations in the activation status of epithelial cells, cells of the innate and adaptive immune response, and the cytokine milieu of the lungs (10, 13, 18, 51).

Despite the relatively abundant information available on the general topic of nematode-malaria co-infections in humans and in animal models (reviewed in (14)), limited attention has been paid to the impact that co-infections have on pulmonary immunity. Hoeve and colleagues simultaneously infected BALB/c mice with *N. brasiliensis* and non-lethal *P. chabaudi chabaudi* and monitored the impact that the malaria-induced Th1 response had on the nature and intensity of a hookworm-induced Th2 response in the lungs (52). In this

experimental design, the effects of co-infection on nematode-induced immunity in the lungs were associated with an attenuated peak expression of Th2 cyokines and markers of M2 activation. This synchronized co-infection had no impact on malaria-induced *IFNg* expression in the lungs. In a second study, where infection with the filarial nematode *Litomosoides sigmodontis* was initiated simultaneously with *P. chabaudi* or *P. yoelii* infection, co-infection had a modulating effect on the intensity of malaria-induced kidney pathology, but no discernable effect on the intensity of malaria-mediated lung damage (53).

In the work presented here, sequential hookworm-malaria infection had a complex influence on the parasitological and morbidity/mortality outcomes of *P. berghei* infection. The presence of the worm-induced Th2 immune environment prior to malaria infection resulted in a modest lag in parasitemia at days 5 and 6 that was accompanied by a paradoxical acceleration in weight loss and trends toward increased mortality and parasite burden in the lungs (Fig. 1A). Previous studies have also reported transient, small, but significant decrements in parasitemia in co-infected animals that could be attributed to in part by the anemia associated with hookworm infection (52, 54). While the trend for an increase in the malaria burden in the lungs in co-infected animals despite a lower parasitemia (Fig. 1A, 1E) could be due to Th2-associated alterations that resulted in increased cytoadherence, it is more likely that inefficient perfusion caused by the *N. brasiliensis*-induced emphysema-like alterations to the lung parenchyma (Fig. 1F) (16, 39) lead to retention of blood in the lungs and the appearance of enhanced sequestration.

Macrophages and monocytes have been shown to play a key role in the innate and adaptive immune response to both hookworm and malaria (15, 22, 37, 44). Previous studies employing the *P. berghei* ANKA-C57BL/6 model of malaria-associated lung injury, demonstrated that cytoadherence of infected erythrocytes to pulmonary post-capillary endothelial surfaces resulted in a robust recruitment of $CCR2^{+}CD11b^{+}Ly6C^{hi}$ monocytes to the lungs starting by day 5 of infection (22). Upon activation in the pulmonary environment, the recruited monocytes were shown to be instrumental in the phagocytic clearance of adherent malaria-infected cells thereby controlling the level of parasite-induced pulmonary inflammation. In notable contrast to the recruited monocytes, lung-resident alveolar macrophages showed no evidence of proliferation or clearance of malaria-infected erythrocytes. This lack of response to malaria challenge by alveolar macrophages is in stark contrast to the ILC2-dependent proliferation and M2 activation induced by the migration of hookworm larvae through the lungs (15, 37, 40, 55).

Consistent with previous reports (15, 37, 40, 55), *N. brasiliensis* infection resulted in an initial increase in the number of macrophages in the alveolar compartment (Fig. 5A) and in the whole lung (Fig. 5B) that later declined leaving behind a population of activated alveolar macrophages (Fig 5D). These activated alveolar macrophages, which were also evident in the BALF from the Nb/Pb group, is emblematic of an altered immune environment that impacted the nature of the innate immune response to malaria in the lung. Starting on day 5 of infection, the levels of M1-like cytokine expression in the lung's macrophage compartment were diminished in Nb/Pb animals compared to the Pb group. Notably, the cells from the Nb/Pb lungs maintained the capacity to respond in an M2-like fashion even in the face of strong M1 polarizing conditions resulting from malaria. This relative lack of

plasticity of lung-associated macrophages is in contrast to the recent findings that *Heligmosomoides polygyrus*-induced IL-4-producing Th2 cells retain functional plasticity and can be induced by a subsequent *P. chabaudi* infection to up-regulate IFNγ production (56). However, dampening the M1 response in the Nb/Pb animals did not have a significant impact on the overall course of the infection.

Of particular note was a significant spike in the transcription of the signature M2 genes Chil3 and Retnla in the CD11c+ cells isolated from the Nb/Pb lungs at day 5. Given the temporally synced expression of these same genes in the Nb group, presumably this increase in M2 gene expression reflects events associated with repair and remodeling mechanisms initiated days earlier in response to the damage and inflammation caused by trafficking of the nematode larvae through the lungs. Indeed, this is a time point where there is a demonstrable progression in the emphysema-like lung destruction that is associated with Nb infection (Fig. 1F) (16, 39, 40).

Though CD11c is a reliable surface marker in mice for lung-resident macrophages, especially alveolar macrophages, it is appreciated that during inflammation additional $CD11c^+$ cells such DCs, activated NK cells, T cells, and B lymphocytes (57) are recruited to the lungs. Our isolation protocol yielded only a small fraction (<5%) of lymphocytic cell types from naive lungs, but following malaria infection, although macrophages/monocytes remained the dominate cell type, the percentage of DC, NK cells, T cells, and B cells increased in a variable fashion in the Pb and Nb/Pb lungs (data not shown). While the expression analysis focused on a suite of genes that encode proteins that are produced by activated macrophages (Fig, 6), we cannot preclude contributions from lymphocytes in these measurements. Additional work will be required to define the relative contributions of different CD11c+ cells to the cytokine response in the lung at days 5 and 8 of malaria infection.

In summary, this work shows for the first time that a recent antecedent helminth infection alters certain aspects of pulmonary immunity to an ensuing malaria infection and underscores that, for the most part, the force exerted on the lung immune response by malaria can rapidly override a pre-existing robust Th2 environment.

Acknowledgments

This work was supported through a pilot grant from the Johns Hopkins Malaria Research Institute (JHMRI) to ALS and NIH grant F32 HL124823 to JMC.

References

1. Bethony J, Brooker S, Albonico M, et al. Soil-transmitted helminth infections: ascariasis, trichuriasis, and hookworm. Lancet. 2006; 367:1521–1532. [PubMed: 16679166]
2. Hotez PJ, Brindley PJ, Bethony JM, King CH, Pearce EJ, Jacobson J. Helminth infections: the great neglected tropical diseases. The Journal of clinical investigation. 2008; 118:1311–1321. [PubMed: 18382743]
3. Savioli L, Albonico M. Soil-transmitted helminthiasis. Nat Rev Microbiol. 2004; 2:618–619. [PubMed: 15303271]

4. Brooker S, Akhwale W, Pullan R, et al. Epidemiology of plasmodium-helminth co-infection in Africa: populations at risk, potential impact on anemia, and prospects for combining control. Am J Trop Med Hyg. 2007; 77:88–98. [PubMed: 18165479]

5. Craig JM, Scott AL. Helminths in the lungs. Parasite Immunol. 2014; 36:463–474. [PubMed: 25201409]

6. Taylor WR, Hanson J, Turner GD, White NJ, Dondorp AM. Respiratory manifestations of malaria. Chest. 2012; 142:492–505. [PubMed: 22871759]

7. Allen JE, Maizels RM. Diversity and dialogue in immunity to helminths. Nat Rev Immunol. 2011; 11:375–388. [PubMed: 21610741]

8. Gaze S, Bethony JM, Periago MV. Immunology of experimental and natural human hookworm infection. Parasite Immunol. 2014; 36:358–366. [PubMed: 25337625]

9. Loke P, MacDonald AS, Robb A, Maizels RM, Allen JE. Alternatively activated macrophages induced by nematode infection inhibit proliferation via cell-to-cell contact. Eur J Immunol. 2000; 30:2669–2678. [PubMed: 11009101]

10. Maizels RM, Yazdanbakhsh M. Immune regulation by helminth parasites: cellular and molecular mechanisms. Nat Rev Immunol. 2003; 3:733–744. [PubMed: 12949497]

11. Mishra PK, Palma M, Bleich D, Loke P, Gause WC. Systemic impact of intestinal helminth infections. Mucosal immunology. 2014; 7:753–762. [PubMed: 24736234]

12. Salgame P, Yap GS, Gause WC. Effect of helminth-induced immunity on infections with microbial pathogens. Nat Immunol. 2013; 14:1118–1126. [PubMed: 24145791]

13. Potian JA, Rafi W, Bhatt K, McBride A, Gause WC, Salgame P. Preexisting helminth infection induces inhibition of innate pulmonary anti-tuberculosis defense by engaging the IL-4 receptor pathway. J Exp Med. 2011; 208:1863–1874. [PubMed: 21825018]

14. Salazar-Castanon VH, Legorreta-Herrera M, Rodriguez-Sosa M. Helminth parasites alter protection against Plasmodium infection. BioMed research international. 2014; 2014:913696. [PubMed: 25276830]

15. Bouchery T, Kyle R, Camberis M, et al. ILC2s and T cells cooperate to ensure maintenance of M2 macrophages for lung immunity against hookworms. Nat Commun. 2015; 6:6970. [PubMed: 25912172]

16. Marsland BJ, Kurrer M, Reissmann R, Harris NL, Kopf M. Nippostrongylus brasiliensis infection leads to the development of emphysema associated with the induction of alternatively activated macrophages. Eur J Immunol. 2008; 38:479–488. [PubMed: 18203142]

17. Reece JJ, Siracusa MC, Southard TL, Brayton CF, Urban JF Jr, Scott AL. Hookworm-induced persistent changes to the immunological environment of the lung. Infect Immun. 2008; 76:3511–3524. [PubMed: 18505812]

18. du Plessis N, Kleynhans L, Thiart L, et al. Acute helminth infection enhances early macrophage mediated control of mycobacterial infection. Mucosal immunology. 2013; 6:931–941. [PubMed: 23250274]

19. Wohlleben G, Trujillo C, Muller J, et al. Helminth infection modulates the development of allergen-induced airway inflammation. Int Immunol. 2004; 16:585–596. [PubMed: 15039389]

20. Fonager J, Pasini EM, Braks JA, et al. Reduced CD36-dependent tissue sequestration of Plasmodium-infected erythrocytes is detrimental to malaria parasite growth in vivo. The Journal of experimental medicine. 2012; 209:93–107. [PubMed: 22184632]

21. Franke-Fayard B, Janse CJ, Cunha-Rodrigues M, et al. Murine malaria parasite sequestration: CD36 is the major receptor, but cerebral pathology is unlinked to sequestration. Proceedings of the National Academy of Sciences of the United States of America. 2005; 102:11468–11473. [PubMed: 16051702]

22. Lagasse HA, Anidi IU, Craig JM, et al. Recruited monocytes modulate malaria-induced lung injury through CD36-mediated clearance of sequestered infected erythrocytes. J Leukoc Biol. 2016; 99:659–671. [PubMed: 26516185]

23. Franke-Fayard B, Janse CJ, Cunha-Rodrigues M, et al. Murine malaria parasite sequestration: CD36 is the major receptor, but cerebral pathology is unlinked to sequestration. Proceedings of the National Academy of Sciences of the United States of America. 2005; 102:11468–11473. [PubMed: 16051702]

24. Amante FH, Haque A, Stanley AC, et al. Immune-mediated mechanisms of parasite tissue sequestration during experimental cerebral malaria. Journal of immunology. 2010; 185:3632–3642.
25. Franke-Fayard B, Waters AP, Janse CJ. Real-time in vivo imaging of transgenic bioluminescent blood stages of rodent malaria parasites in mice. Nature protocols. 2006; 1:476–485. [PubMed: 17406270]
26. Lovegrove FE, Gharib SA, Pena-Castillo L, et al. Parasite burden and CD36-mediated sequestration are determinants of acute lung injury in an experimental malaria model. PLoS pathogens. 2008; 4:e1000068. [PubMed: 18483551]
27. Taylor JJ, Krawczyk CM, Mohrs M, Pearce EJ. Th2 cell hyporesponsiveness during chronic murine schistosomiasis is cell intrinsic and linked to GRAIL expression. J Clin Invest. 2009; 119:1019–1028. [PubMed: 19258704]
28. Crompton PD, Moebius J, Portugal S, et al. Malaria immunity in man and mosquito: insights into unsolved mysteries of a deadly infectious disease. Annu Rev Immunol. 2014; 32:157–187. [PubMed: 24655294]
29. Langhorne J, Ndungu FM, Sponaas AM, Marsh K. Immunity to malaria: more questions than answers. Nat Immunol. 2008; 9:725–732. [PubMed: 18563083]
30. van den, Ham HJ., Andeweg, AC., de Boer, RJ. Induction of appropriate Th cell phenotypes: Cellular decision-making in heterogeneous environments. Parasite Immunol. 2013
31. Adegnika AA, Kremsner PG. Epidemiology of malaria and helminth interaction: a review from 2001 to 2011. Current opinion in HIV and AIDS. 2012; 7:221–224. [PubMed: 22418449]
32. Hartgers FC, Yazdanbakhsh M. Co-infection of helminths and malaria: modulation of the immune responses to malaria. Parasite Immunol. 2006; 28:497–506. [PubMed: 16965285]
33. Knowles SC. The effect of helminth co-infection on malaria in mice: a meta-analysis. Int J Parasitol. 2011; 41:1041–1051. [PubMed: 21777589]
34. Camberis, M., Le Gros, G., Urban, J, Jr. Animal model of Nippostrongylus brasiliensis and Heligmosomoides polygyrus. In: Coligan, John E., et al., editors. Current protocols in immunology. 2003. Chapter 19: Unit 19 12
35. Lee MA, Tan CH, Aw LT, et al. Real-time fluorescence-based PCR for detection of malaria parasites. J Clin Microbiol. 2002; 40:4343–4345. [PubMed: 12409427]
36. Goman M, Langsley G, Hyde JE, Yankovsky NK, Zolg JW, Scaife JG. The establishment of genomic DNA libraries for the human malaria parasite Plasmodium falciparum and identification of individual clones by hybridisation. Mol Biochem Parasitol. 1982; 5:391–400. [PubMed: 6213858]
37. Siracusa MC, Reece JJ, Urban JF Jr, Scott AL. Dynamics of lung macrophage activation in response to helminth infection. Journal of leukocyte biology. 2008; 84:1422–1433. [PubMed: 18719016]
38. Anidi IU, Servinsky LE, Rentsendorj O, Stephens RS, Scott AL, Pearse DB. CD36 and Fyn Kinase Mediate Malaria-Induced Lung Endothelial Barrier Dysfunction in Mice Infected with Plasmodium berghei. PLoS One. 2013; 8:e71010. [PubMed: 23967147]
39. Heitmann L, Rani R, Dawson L, et al. TGF-beta-responsive myeloid cells suppress type 2 immunity and emphysematous pathology after hookworm infection. Am J Pathol. 2012; 181:897–906. [PubMed: 22901754]
40. Turner JE, Morrison PJ, Wilhelm C, et al. IL-9-mediated survival of type 2 innate lymphoid cells promotes damage control in helminth-induced lung inflammation. J Exp Med. 2013; 210:2951–2965. [PubMed: 24249111]
41. Perez-Mazliah D, Langhorne J. CD4 T-cell subsets in malaria: TH1/TH2 revisited. Frontiers in immunology. 2014; 5:671. [PubMed: 25628621]
42. Villegas-Mendez A, de Souza JB, Murungi L, et al. Heterogeneous and tissue-specific regulation of effector T cell responses by IFN-gamma during Plasmodium berghei ANKA infection. J Immunol. 2011; 187:2885–2897. [PubMed: 21880980]
43. Stevenson MM, Riley EM. Innate immunity to malaria. Nature reviews Immunology. 2004; 4:169–180.

44. Borthwick LA, Barron L, Hart KM, et al. Macrophages are critical to the maintenance of IL-13-dependent lung inflammation and fibrosis. Mucosal immunology. 2016; 9:38–55. [PubMed: 25921340]
45. Josefowicz SZ, Lu LF, Rudensky AY. Regulatory T cells: mechanisms of differentiation and function. Annu Rev Immunol. 2012; 30:531–564. [PubMed: 22224781]
46. Maizels RM, Yazdanbakhsh M. Immune regulation by helminth parasites: cellular and molecular mechanisms. Nature reviews Immunology. 2003; 3:733–744.
47. Hansen DS, Schofield L. Natural regulatory T cells in malaria: host or parasite allies? PLoS Pathog. 2010; 6:pe1000771.
48. Pot C, Jin H, Awasthi A, et al. Cutting edge: IL-27 induces the transcription factor c-Maf, cytokine IL-21, and the costimulatory receptor ICOS that coordinately act together to promote differentiation of IL-10-producing Tr1 cells. J Immunol. 2009; 183:797–801. [PubMed: 19570826]
49. Sheppard D. Transforming growth factor beta: a central modulator of pulmonary and airway inflammation and fibrosis. Proceedings of the American Thoracic Society. 2006; 3:413–417. [PubMed: 16799084]
50. Griffith JW, Sun T, McIntosh MT, Bucala R. Pure Hemozoin is inflammatory in vivo and activates the NALP3 inflammasome via release of uric acid. J Immunol. 2009; 183:5208–5220. [PubMed: 19783673]
51. Didierlaurent A, Goulding J, Hussell T. The impact of successive infections on the lung microenvironment. Immunology. 2007; 122:457–465. [PubMed: 17991012]
52. Hoeve MA, Mylonas KJ, Fairlie-Clarke KJ, Mahajan SM, Allen JE, Graham AL. Plasmodium chabaudi limits early Nippostrongylus brasiliensis-induced pulmonary immune activation and Th2 polarization in co-infected mice. BMC Immunol. 2009; 10:60. [PubMed: 19951425]
53. Karadjian G, Berrebi D, Dogna N, et al. Co-infection restrains Litomosoides sigmodontis filarial load and plasmodial P. yoelii but not P. chabaudi parasitaemia in mice. Parasite. 2014; 21:16. [PubMed: 24717449]
54. Griffiths EC, Fairlie-Clarke K, Allen JE, Metcalf CJ, Graham AL. Bottom-up regulation of malaria population dynamics in mice co-infected with lung-migratory nematodes. Ecology letters. 2015; 18:1387–1396. [PubMed: 26477454]
55. Huber S, Hoffmann R, Muskens F, Voehringer D. Alternatively activated macrophages inhibit T-cell proliferation by Stat6-dependent expression of PD-L2. Blood. 2010; 116:3311–3320. [PubMed: 20625006]
56. Coomes SM, Pelly VS, Kannan Y, et al. IFNgamma and IL-12 Restrict Th2 Responses during Helminth/Plasmodium Co-Infection and Promote IFNgamma from Th2 Cells. PLoS Pathog. 2015; 11:e1004994. [PubMed: 26147567]
57. Guth AM, Janssen WJ, Bosio CM, Crouch EC, Henson PM, Dow SW. Lung environment determines unique phenotype of alveolar macrophages. American journal of physiology Lung cellular and molecular physiology. 2009; 296:L936–946. [PubMed: 19304907]

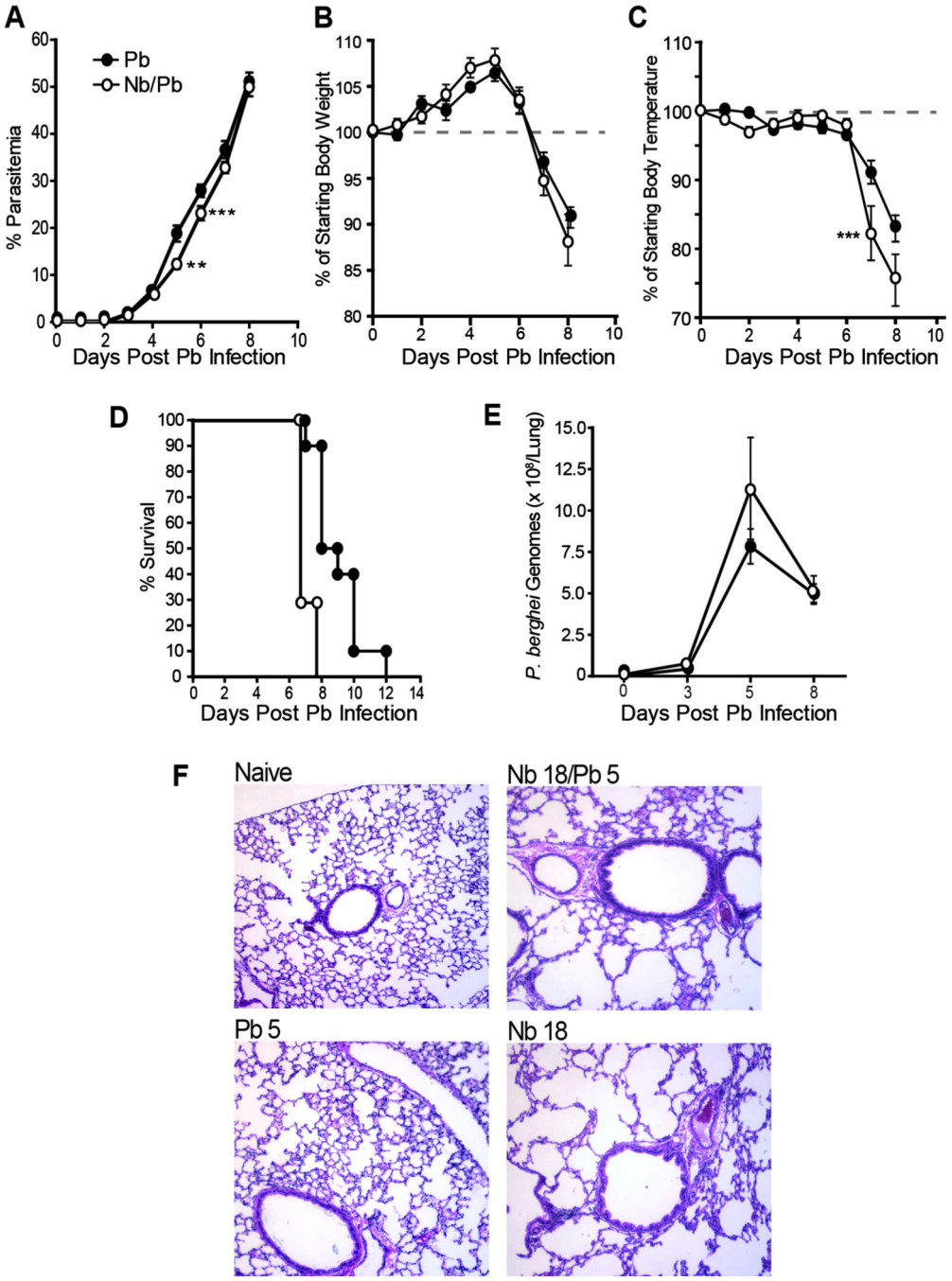

Figure 1.

Impact of prior *N. brasiliensis* exposure on parasitemia, morbidity and parasite sequestration in the lungs during *P. berghei* infection. (A) Peripheral blood parasitemia, (B) change in weight, (C) change in temperature, and (D) survival in mice infected with *P. berghei* alone (Pb) or with malaria 13 days following infection with *N. brasiliensis* (Nb/Pb) at 0, 3, 5, and 8 days after the initiation of malaria infection. (E) The number of *P. berghei* genomes in perfused lung tissue as measured by real-time PCR for Pb 18s rRNA expression. (F) Representative H&E-stained lung sections (10x magnification) 5 days from Pb or Nb/Pb

groups. Data points show mean ± SEM derived from 10 Pb-infected BALB/cJ mice or 7 Nb/Pb-infected BALB/cJ mice. ** = $p < 0.01$, *** = $p < 0.001$ by two-way ANOVA (A–C) or log-rank test (D) comparing Nb/Pb to Pb.

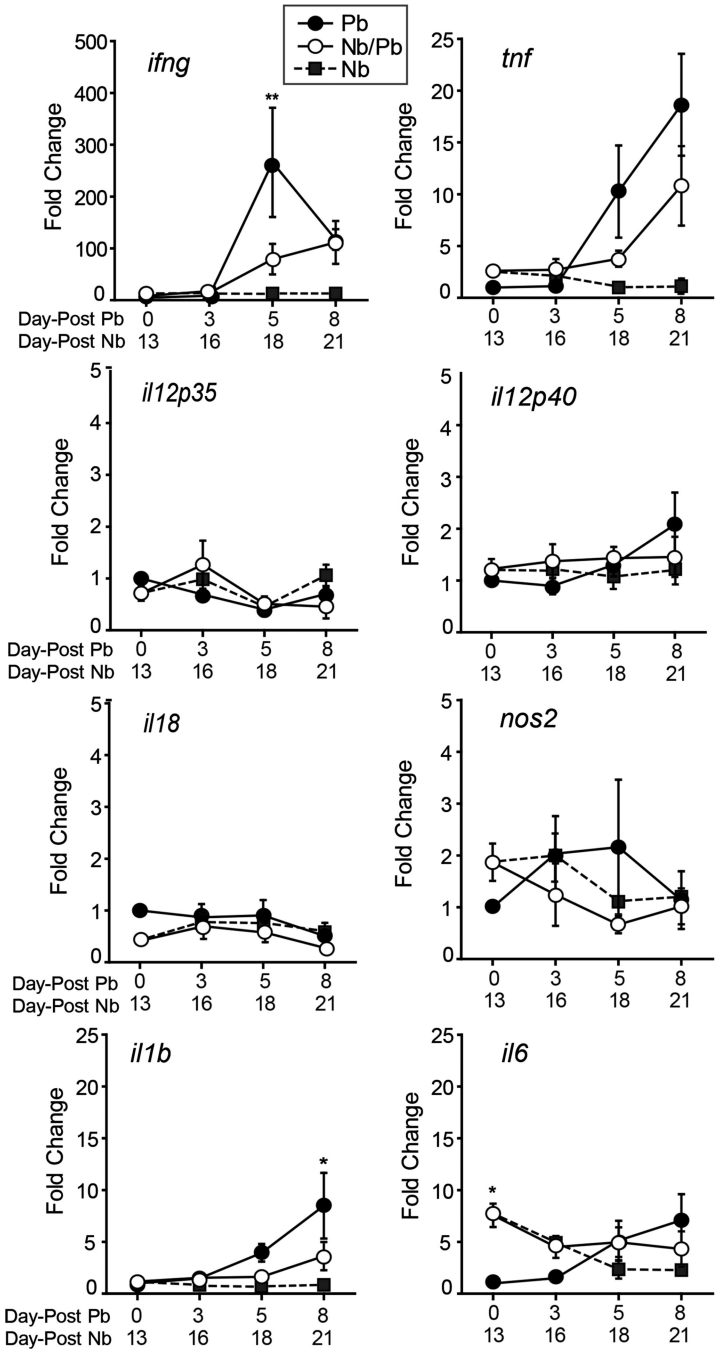

Figure 2.

Impact of prior *N. brasiliensis* exposure on the expression of Th1-associated cytokine genes in the lungs during *P. berghei* infection. Real-time RT-PCR analysis of mRNA levels of *ifng, tnf, il12p35, il12p40, il18, nos2, il1b*, and *il6* in the lungs isolated from mice infected with *P. berghei* alone (Pb), *N. brasiliensis* alone (Nb), or with hookworm 13 days prior to malaria (Nb/Pb) at 0, 3, 5, and 8 days after the initiation of malaria infection. Data points are mean fold change in transcription over that of naive Day 0 mice normalized to GAPDH ± SEM, N

= 5 wild-type BALB/cJ male mice. ** = $p < 0.01$ by two-way ANOVA comparing Nb/Pb to Pb.

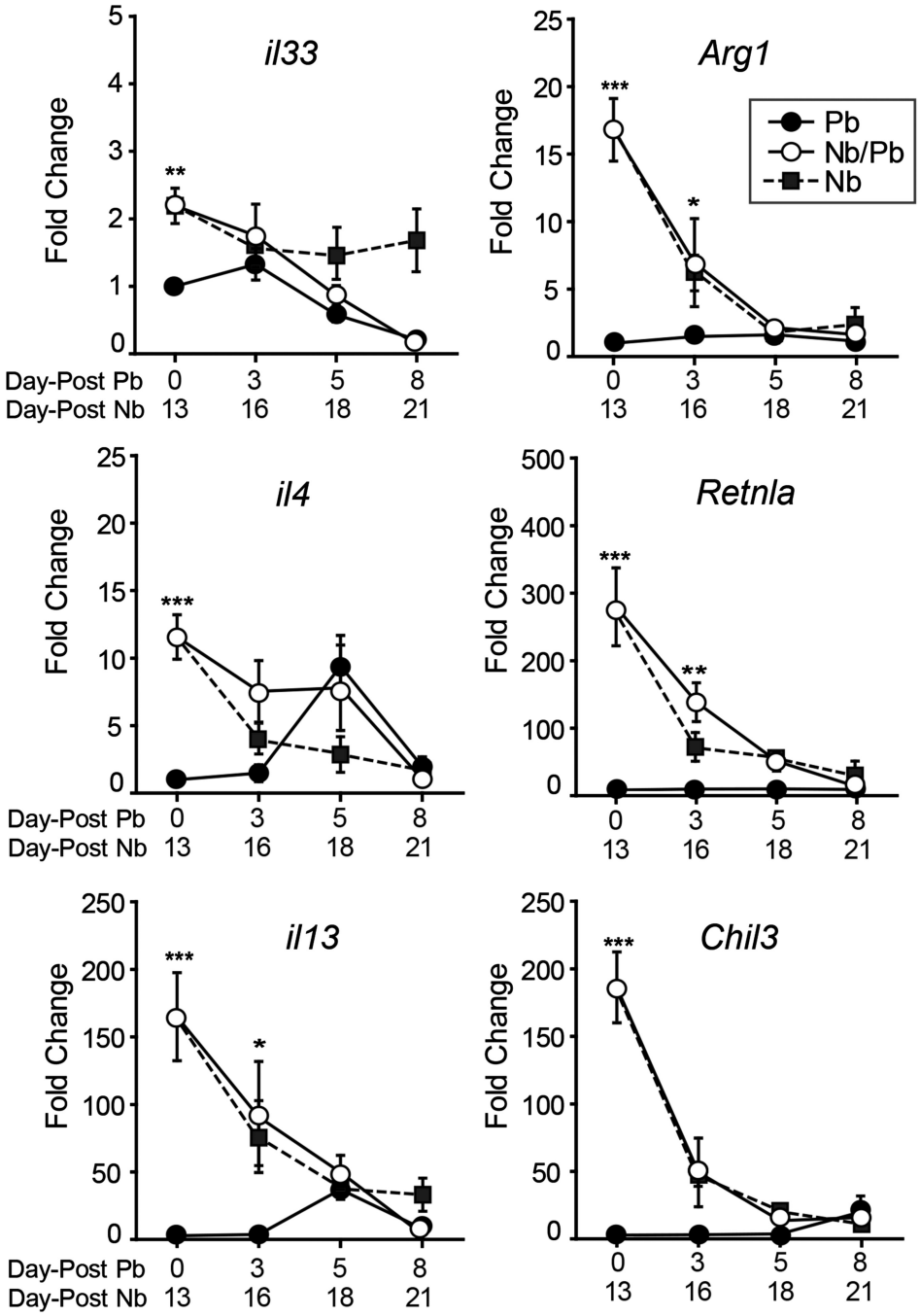

Figure 3.

Impact of a *P. berghei* infection on the Th2-associated cytokine gene expression induced by a prior *N. brasiliensis* infection. Real-time RT-PCR analysis of mRNA levels of *il33, arg1, il4, retnla, il13*, and *chil3* in the lungs isolated from mice infected with *P. berghei* alone (Pb), *N. brasiliensis* alone (Nb), or with hookworm 13 days prior to malaria (Nb/Pb) at 0, 3, 5, and 8 days after the initiation of malaria infection. Data points show mean fold change over naive Day 0 mice normalized to GAPDH ± SEM derived from 5 wild-type BALB/cJ mice. * = $p < 0.05$, ** = $p < 0.01$, *** = $p < 0.001$ by two-way ANOVA comparing Nb/Pb to Pb.

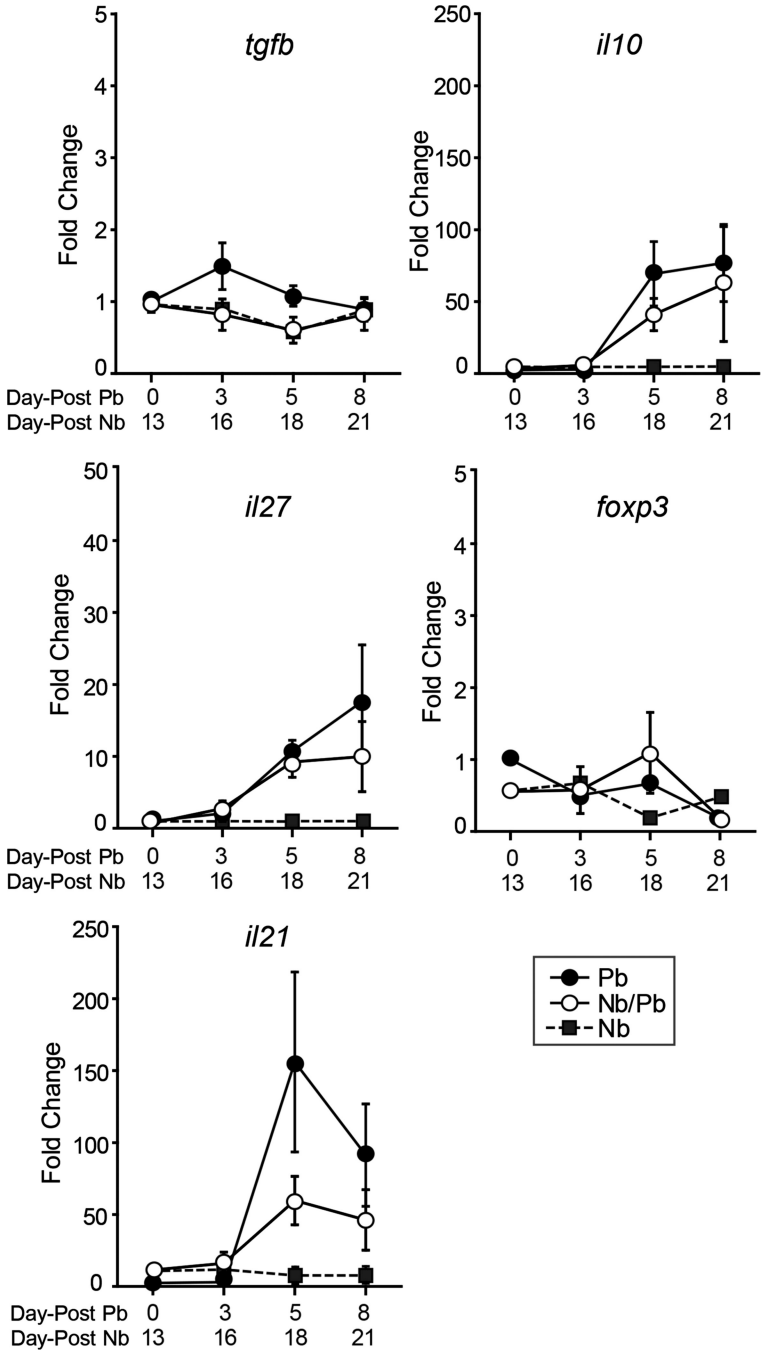

Figure 4.

Hookworm infection does not significantly impact the expression of Treg-associated cytokine genes in the lungs during a subsequent malaria infection. Real-time RT-PCR analysis of mRNA levels of *tgfb*, *il10, il27, foxp3*, and *il21* in the lungs isolated from mice infected with *P. berghei* alone (Pb), *N. brasiliensis* alone (Nb), or with hookworm 13 days prior to malaria (Nb/Pb) at 0, 3, 5, and 8 days after the initiation of malaria infection. Data points show mean fold change over naive Day 0 mice normalized to GAPDH ± SEM derived

from 5 wild-type BALB/cJ mice. Nb/Pb compared to Pb not significantly different by two-way ANOVA.

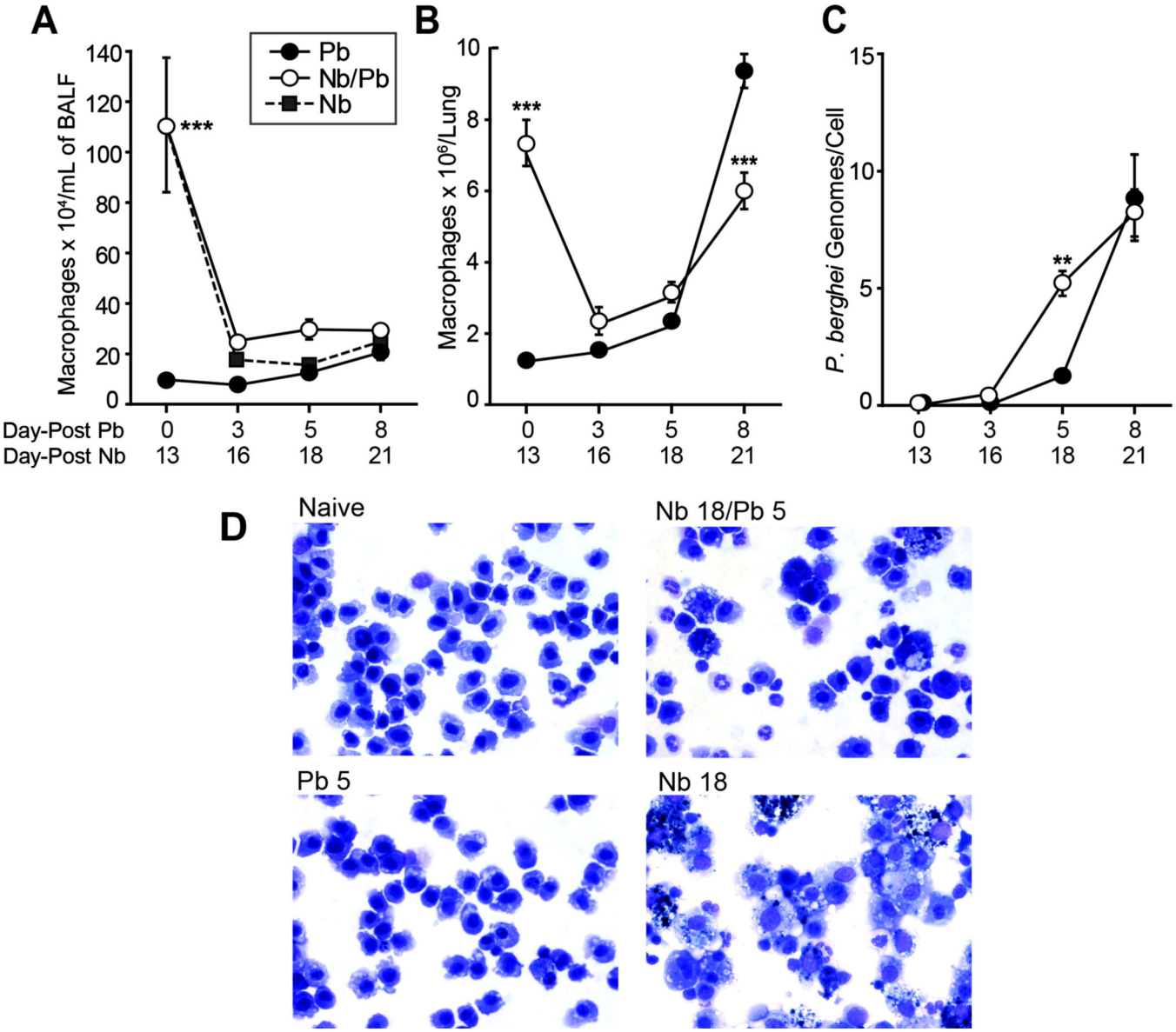

Figure 5.

Impact of prior *N. brasiliensis* exposure on lung macrophage dynamics and appearance in the lungs during *P. berghei* infection. The number of macrophages in recovered bronchoalveolar lavage fluid (BALF) (A) or from whole lungs (B) from mice infected with *P. berghei* alone (Pb), *N. brasiliensis* alone (Nb), or with hookworm 13 days prior to malaria (Nb/Pb) at 0, 3, 5, and 8 days after the initiation of malaria infection. (C) The number of *P. berghei* genomes per isolated $CD11c^{+}$ cell as measured by real-time PCR for Pb 18s rRNA expression. Data points show mean ± SEM derived from 3 wild-type BALB/cJ mice. * = $p < 0.05$, *** = $p < 0.001$ by two-way ANOVA comparing Nb/Pb to Pb. (D) Representative Diff-Quik-stained BAL samples 5 days after infection with Pb or Nb/Pb compared to a naive Day 0 sample (60x magnification).

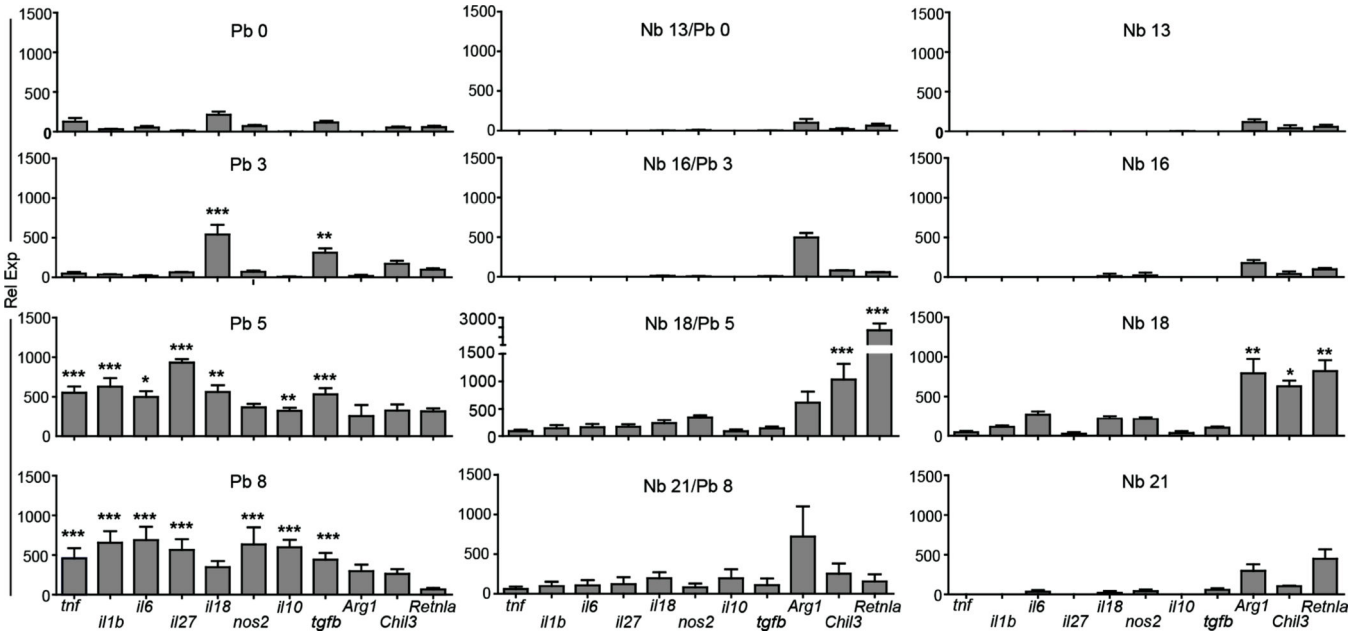

Figure 6.

Impact of prior *N. brasiliensis* exposure on cytokine expression the CD11C+ cell subset in the lungs during *P. berghei* infection. Real-time RT-PCR analysis of mRNA levels for the genes encoding TNF-α, IL-1β, IL-6, IL-27, IL-18, NOS2, IL-10, TGF-β, Arg1, Ym1, and Fizz1 in lung CD11c+ cells isolated at Days 0, 3, 5, and 8 after infection with *P. berghei* alone (Pb), *N. brasiliensis* alone (Nb), or with malaria 13 days after infection with *N. brasiliensis* (Nb/Pb). Bars show mean relative expression normalized to GAPDH ± SEM derived from 5 BALB/cJ mice/group. * = $p < 0.05$, ** = $p < 0.01$, *** = $p < 0.001$ by two-way ANOVA comparing Nb/Pb to Pb.